

# Technoeconomic Analysis of a Hybrid Biomass Thermochemical and Electrochemical Conversion System

Qi Dang,<sup>[a, b]</sup> Mark Mba Wright,<sup>\*[a, b]</sup> and Wenzhen Li<sup>[c]</sup>

This study explores an integrated biomass conversion system based on a common fast pyrolysis step and two subsequent bio-oil upgrading pathways. The two options are bio-oil thermochemical upgrading to drop-in transportation biofuels through hydrotreating and hydrocracking, and bio-oil electrochemical conversion for electrical power generation using a direct bio-oil fuel cell method. The technoeconomic performances of biomass-to-biofuels and biomass-to-electricity pathways are first examined individually, and then integrated for the analysis of a hybrid biomass conversion system. A biomass facility of 2000 tonnes per day is investigated as a baseline. The minimum fuel-selling price (MFSP) is estimated to be \$2.48 per gallon, with biomass feedstock and other

operating costs as major contributors. A very high minimum electricity-selling price (MESP) of \$5.36 per kWh is projected based on the current laboratory-scale fuel cell configuration. Sensitivity analysis reveals that the effective reactant content in bio-oil, the degree of oxidation, and the fuel cell system efficiency play key roles in the MESP. The estimate can be reduced to \$0.96 per kWh if target values of the three parameters are met. The results of the hybrid system suggest that the MESP can be reduced substantially from \$0.96 to \$0 per kWh when the hybrid system increases the bio-oil fraction for biofuel production from 0 to 75.8%, given a bio-fuel MFSP of \$3 per gallon.

## Introduction

Global concerns over the long-term availability and sustainability of energy resources have led scientists to develop renewable alternatives to fossil-based fuels. Biomass is an attractive renewable alternative to fossil fuels due to its ability to reduce carbon emissions and enhance energy security. It can be processed in various ways, such as fermentation, combustion, gasification, pyrolysis, and electrochemical conversion pathways, to produce fuel and energy.<sup>[1–3]</sup> Among these biomass conversion options, fast pyrolysis shows promise as a low-cost pathway to renewable fuel and chemical production.<sup>[4,5]</sup> Electrochemical conversion technologies have shown extensive applications in energy storage and generation devices due to their efficiency in conversion and utilization of renewable carbon sources.<sup>[6,7]</sup>

Fast pyrolysis is a thermochemical decomposition process that converts a variety of biomass feedstocks into bio-oil with noncondensable gas (NCG) and solid biochar by-products.<sup>[8]</sup> The thermochemical reaction takes place at temperatures of about 500 °C and residence times on the order of seconds. The reaction yields bio-oil with a composition determined by the properties of the feedstocks, reaction conditions, and the effect of catalysts. Hundreds of oxygenated compounds have been identified in bio-oil.<sup>[9,10]</sup> These compounds can be recovered as distilled fractions with distinct properties and upgraded by using appropriate downstream facilities to produce biofuels, chemicals, biobased products, and electrical power.<sup>[5,11]</sup> Substantial efforts have been devoted to this research field, as evidenced by a growing number of publications on experimental investigations and the technoeconomics of biomass fast pyrolysis systems. In particular,

there is growing interest in the integrated fast pyrolysis biorefinery concept for the coproduction of fuels and chemicals. Hu et al. compared the technoeconomic performance of a fast pyrolysis biorefinery for the production of hydrocarbon biofuels, biobased products, and hydrocarbon chemicals.<sup>[11]</sup> Li et al. explored, in particular, the economic feasibility of producing gasoline and diesel from biomass fast pyrolysis and hydrotreating and hydrocracking.<sup>[12]</sup> Dang et al. investigated the use of a mixture of bio-oil and coal as a substitute for boiler fuel in power plants for electricity generation from both environmental and economic perspectives.<sup>[13]</sup>

Electrochemical energy conversion is a developing approach to utilize renewable carbon resources, such as bio-oil derived from biomass fast pyrolysis. Bio-oil can be potentially upgraded into electrical power, higher value chemicals, and biobased products through various electrochemical conversion devices.<sup>[14]</sup> A fuel cell is one type of device to directly convert chemical energy into electricity. It offers a clean and

[a] Dr. Q. Dang, Prof. Dr. M. M. Wright  
Bioeconomy Institute, Iowa State University  
Ames, IA 50011 (USA)  
E-mail: markmw@iastate.edu

[b] Dr. Q. Dang, Prof. Dr. M. M. Wright  
Department of Mechanical Engineering  
Iowa State University, Ames, IA 50011 (USA)

[c] Prof. Dr. W. Li  
Department of Chemical & Biological Engineering  
Iowa State University, Ames, IA 50011 (USA)

Supporting Information and the ORCID identification number(s) for the author(s) of this article can be found under <https://doi.org/10.1002/ente.201700395>.

efficient way for power generation from renewable carbon sources. A variety of carbon sources, such as glucose, fructose, and glycerol, have been widely explored by researchers with a focus on alkaline fuel cell configurations.<sup>[15–18]</sup> Fujiwara et al. tested the performance of nonenzymatic glucose fuel cells by using anion-exchange membranes.<sup>[15]</sup> A peak power density of  $20 \text{ mW cm}^{-2}$  was delivered with  $0.5 \text{ M}$  D-glucose in a  $0.5 \text{ M}$  solution of KOH with an anion-exchange membrane. Basu and Basu compared direct glucose and fructose alkaline fuel cells.<sup>[16]</sup> A maximum peak power density of  $1.38 \text{ mW cm}^{-2}$  was reported with  $0.2 \text{ M}$  glucose in  $1 \text{ M}$  KOH at  $30^\circ\text{C}$  and Pt–Ru/C as an anode catalyst. The peak power density was reduced with the operation of fructose. Li et al. investigated the electro-oxidation of glycerol with an anion-exchange membrane in a flow reactor.<sup>[19,20]</sup> The selectivity of chemicals produced from glycerol oxidation was studied with different catalysts and various operating conditions. Lam et al. analyzed the electrocatalytic hydrogenation of fast pyrolysis bio-oil as an immediate stabilization strategy for the sustainable production of hydrocarbon fuels.<sup>[14]</sup> Most of these studies focus on the electrocatalytic oxidation of pure biomass-derived model compounds in fuel cell applications for simplicity and high efficiency.

In more recent work, Benipal et al. reported, for the first time, the successful application of fast pyrolysis bio-oil as a fuel in an alkaline anion-exchange membrane fuel cell for renewable electrical power production.<sup>[21]</sup> They investigated the impacts of catalyst types, operating temperatures, KOH concentrations, and bio-oil concentrations on the performance of fuel cells in a laboratory batch-scale reactor. An optimal peak power density of  $42.7 \text{ mW cm}^{-2}$  was observed with a solution of  $30 \text{ wt}\%$  bio-oil and  $6.0 \text{ M}$  KOH with palladium as an anode catalyst. This direct bio-oil fuel cell technology is currently undergoing laboratory-scale testing and further research and development are required before it becomes mature and ready for widespread deployment. This makes the investigation of its techno-economic potential for long-term success of particular interest and the focus of this study. There is scarce information on the techno-economic analysis of biofuel-based fuel cell technologies and direct bio-oil fuel cells specifically, but studies on the cost analysis of other types of fuel cells can be found in the literature for comparison purposes.<sup>[22–24]</sup>

We propose herein that bio-oil produced from biomass fast pyrolysis could be potentially utilized in two ways, in which it can either be upgraded in a biorefinery for transportation biofuel production or utilized in novel fuel cell technology for electrical power generation. The traditional way of using bio-oil for heat and power generation and other conversion pathways is not analyzed herein, with the intention that new advanced technologies will potentially be commercialized and widely employed in the future. This work covers cost analysis methods for both the biomass thermochemical conversion pathway (biofuel production from a fast pyrolysis biorefinery) and biomass electrochemical conversion pathway (electrical power generation from direct bio-oil fuel cells), with a focus on the latter. Furthermore, this study is

extended to analyze the overall economics of a hybrid biomass processing system in which both electricity and biofuels are generated from bio-oil. The minimum electricity-selling price (MESP) of the hybrid system is evaluated. The challenges and cost-reduction opportunities associated with this novel direct bio-oil fuel cell technology are identified.

## Methodology

### Description of biofuel production pathways

Fast pyrolysis of biomass produces bio-oil as an intermediate, which can be further upgraded to a blend of gasoline and diesel for transportation use. The techno-economic analysis of biomass fast pyrolysis to gasoline and diesel has been explored by many researchers.<sup>[25,26]</sup> This work builds upon our previous Aspen Plus™ models and papers in which we analyzed a fast pyrolysis biorefinery with an input of 2000 tonnes per day of red oak biomass.<sup>[5,11,12]</sup> The overall conversion route covers biomass pretreatment (drying and grinding), fast pyrolysis (at  $500^\circ\text{C}$  in a fluidized-bed reactor), bio-oil fractionation (five-stage fractionation system), stabilization (a two-stage hydrotreating step), upgrading (hydrocracking), and hydrogen generation sections (steam reforming of light ends of bio-oil and natural gas). The bio-oil stabilization unit consists of a two-step hydrotreatment process, whereas upgrading refers to hydrocracking of high-molecular-weight compounds and distillation to gasoline and diesel.

### Cost estimate for biofuels

Wright and Brown introduced a simplified methodology to calculate the production cost of biofuels and proposed a way to incorporate the effect of economies of scale.<sup>[27]</sup> Herein, we adapt and apply a similar method for our estimate. The core part of the cost analysis is to assess the capital and operating costs, and thus, obtain the minimum fuel-selling price (MFSP) estimate. The costs in the following description are reported in US dollars for data from 2011.

With a biorefinery processing  $M_0$  tonnes of biomass per day (MTPD), the total annual cost for biofuel production,  $C_{T0}$ , can be broken down into annual capital cost, feedstock cost, feedstock delivery cost, and other costs, as indicated in Equation (1):

$$C_{T0} = C_{P0} + C_{F0} + C_{D0} + C_{E0} + C_{O0} - C_{r_{bc0}} \quad (1)$$

in which  $C_{P0}$  is the annual capital cost;  $C_{F0}$  is the feedstock cost;  $C_{D0}$  is the feedstock delivery cost;  $C_{E0}$  is the material/energy cost of bio-oil production, including electricity consumption for biomass grinding and fast pyrolysis;  $C_{O0}$  is the lump material/energy cost associated with bio-oil upgrading for biofuel production, mainly including purchased electricity, natural gas, and catalyst costs; and  $C_{r_{bc0}}$  represents the credits from biochar. A previous study indicated that 52% of produced biochar was combusted to provide energy for the fast pyrolysis process and biomass drying, whereas the re-

maining biochar could be sold at a market price of \$20 per tonne based on its heating value as a substitute for coal. The annual capital cost,  $C_{P0}$ , is obtained by assigning a recovery factor,  $\text{irr}/[1-\exp(-\text{irr}t_{\text{bp}})]$  to the total fixed capital cost of the biorefinery based on continuous payment and compounding across the lifetime of the biorefinery,<sup>[28]</sup> in which “irr” is the internal rate of return and  $t_{\text{bp}}$  is the lifetime of the biorefinery. A 10% internal rate of return and 30 year plant life is used. The fixed capital cost of the biorefinery is obtained by multiplying the total purchased equipment cost by a given Lang factor. The total purchased equipment cost, including pretreatment and pyrolysis, fractionation, stabilization, upgrading, and steam reforming of natural gas for hydrogen generation, is taken from our previous study,<sup>[5]</sup> in which pretreatment and pyrolysis and hydrogen generation were found to be significant contributors. The feedstock price is assumed to be \$80 per tonne for red oak. The biomass delivery cost can be assessed according to the equations in Ref. [27], given the unit cost for feedstock delivery, the average delivery distance, and the amount of biomass delivered to the biorefinery. This calculation takes into account inputs of a biomass delivery unit at a cost of \$0.71 per ton per mile, a biomass annual yield of 5 tonnes per acre, and a 60% acreage around the biorefinery devoted to feedstock production. Once the individual components of Equation (1) are achieved, the total annual cost of the biorefinery,  $C_{T0}$ , is obtained and the MFSP can be calculated by dividing  $C_{T0}$  by the annual biofuel production with a quantity of  $Q_0$  in million gallons. The key parameters and assumptions used for the MFSP estimate are summarized in Table 1.

When evaluating a biorefinery with a new processing capacity of  $M$ , the total annual cost for biofuel production can be estimated with respect to the baseline case data. Because the fixed capital cost of biorefineries is driven by economics of scale in general, the capital cost of the new facility scales with that of the baseline biorefinery with a power law exponent  $n$ ; a value of 0.7 is used for biorefineries.<sup>[27,29]</sup> The biomass delivery cost is scaled with another power law exponent  $m$ , which is set to be 1.5 in most cases.<sup>[27]</sup> The feedstock and other material related costs adopt a linear scaling factor, and thus, the cost of the new biorefinery can be calculated from

Equation (2). The new MFSP is estimated with a known biofuel quantity of  $Q$  in million gallons per year. This cost method gives us a simplified way to estimate MFSP and enables us to capture the cost variation with different biorefinery capacities.

$$C_T = C_{P0} \left(\frac{M}{M_0}\right)^n + C_{D0} \left(\frac{M}{M_0}\right)^m + (C_{F0} + C_{O0} + C_{E0} - C_{r_{\text{bc0}}}) \left(\frac{M}{M_0}\right) \quad (2)$$

### Performance of the direct bio-oil fuel cell

Fuel cells are typically characterized by key parameters, such as power density, current density, voltage, efficiencies, and power capacity. The intrinsic performance is determined by electrochemical reactions. In terms of evaluating the performance of the direct bio-oil fuel cell, Benipal et al. explored various operating conditions by optimizing critical parameters, such as catalysts, operating temperatures, bio-oil concentrations, and KOH concentrations with an electrode active area of  $5 \text{ cm}^2$ .<sup>[21]</sup> The optimal performance is revealed when a solution of 30 wt% bio-oil and 6M KOH are fed into the anode at a flow rate of  $4 \text{ mL min}^{-1}$ , as air flows through the cathode. A peak power density of  $42.7 \text{ mW cm}^{-2}$  is delivered with a palladium catalyst, which corresponds to a current density of  $180.3 \text{ mA cm}^{-2}$  and a voltage of 0.23 V. The optimal performance forms the basis for this analysis. Compared with the current laboratory-scale setup, an active area of  $236.5 \text{ cm}^2$  per cell and 369 cells in each stack are employed to better represent the large-scale application of direct bio-oil fuel cells for stationary power generation with reference to a report by Directed Technologies, Inc.<sup>[30]</sup> A larger fuel cell stack design indicates more fuel consumption, while the performance of direct bio-oil fuel cells stay the same. Experimental data and design parameters of fuel cell stacks are presented in Table 2. Based on the power density, active area per stack, and system efficiency, considering the parasitic loss and inverter loss, the stack power output capacity,  $P_{\text{net}}$ , can be calculated.

### Cost estimate for electricity

The fuel cell stack is aggregated by different components, and thus, it allows for a component-level cost analysis. In general, the capital cost of a direct bio-oil fuel stack module consists of the stack cost, the balance of plant cost, and the system assembly and testing cost, as described in Equation (3).

$$c_p = c_s + c_{\text{bop}} + c_a \quad (3)$$

in which  $c_p$  is the total capital cost of a stack in \$,  $c_s$  is the stack cost in \$,  $c_{\text{bop}}$  is the balance of plant cost in \$, and  $c_a$  is the system assembly and testing cost in \$. The stack cost in-

**Table 1.** Key parameters and assumptions for the fast pyrolysis biofuel pathway.

Parameter	Value
biomass [MTPD]	2000
biomass price [\$/tonne]	80
bio-oil yield based on biomass [wt%]	65.9
biofuel yield based on biomass [gallon per ton biomass]	86.5
annual operating hours [h]	7884
total purchased equipment cost [\$ MM] <sup>[a]</sup>	67.5
Lang factor	4.69
internal rate of return	0.1
plant life [year]	30
capital recovery factor	0.105

[a] \$ MM = Million.

**Table 2.** Performance characteristics and key parameters of a direct bio-oil fuel cell.

Parameter	Value	Ref.
current density [ $\text{mAcm}^{-2}$ ]	180.3	[21]
V [V]	0.23	[21]
power density [ $\text{mWcm}^{-2}$ ]	42.7	[21]
area per cell [ $\text{cm}^2$ ]	5	[21]
system efficiency	0.92	[30]
fuel for anode	30 wt% bio-oil + 6.0M KOH	[21]
pump flow rate [ $\text{mLmin}^{-1}$ ]	4	[21]
KOH consumption factor [%]	0.5	
KOH price [ $\text{\$ kg}^{-1}$ ]	1	[31]
Pd anode catalyst loading [ $\text{mgcm}^{-2}$ ]	0.5	[21]
Fe cathode catalyst loading [ $\text{mgcm}^{-2}$ ]	3	[21]
Pd price [ $\text{\$ g}^{-1}$ ]	35.4	[30]
Fe price [ $\text{\$ kg}^{-1}$ ]	27.6	[32]
fuel cell operating hours [h]	7884	
fuel cell lifetime [year]	3	adapted from [23, 33]
internal rate of return	0.1	
capital recovery factor	0.386	
active area per cell [ $\text{cm}^2$ ]	236.5	[30]
no. cells per stack	369	[30]

cludes stamped bipolar plates, membrane electrode assemblies (MEAs), coolant gaskets, end gaskets, end plates, current collectors, compression bands, stack housing, stack assembly, and stack conditioning. MEAs are the core part of the stack. The nanostructured thin-film catalyst deposition process is applied for the production of MEAs. Component  $c_s$  in Equation (3) is divided into the cost of the catalyst material and the total cost of the remaining stack components to account for the impact of catalyst loadings on the electricity selling prices. The balance of plant cost covers the air loop, humidifier and water recovery loop, high-temperature coolant loop, low-temperature coolant loop, fuel loop, system controllers, sensors, and miscellaneous. The net power output from each fuel cell stack is represented by  $P_{\text{net}}$ , and thus, the stack production cost on a net power output basis is expressed as  $c_p/P_{\text{net}}$  in  $\text{\$ kW}^{-1}$ .

The novel application of direct bio-oil fuel cells is still in an early development stage and no commercial data is publicly available with respect to the cost of the specific design. Due to this limitation, we refer to the stack cost of a hydrogen proton-exchange membrane ( $\text{H}_2$  PEM) fuel cell system reported by James et al.,<sup>[30]</sup> who detailed a component-level analysis, including material, manufacturing, and tooling costs, with an annual production rate of 30 000 stacks. Though in reality the cost and design structure of a bio-oil direct fuel cell system are different from those of  $\text{H}_2$  PEM fuel cells (due to the particular properties of bio-oil), at this point, we chose the cost information for  $\text{H}_2$  PEM fuel as the analysis reference, with the vision that the cost of commercial bio-oil fuel cells would approach that of the reference. It is worth noting that the specific catalyst types and loadings, and the performance of the direct bio-oil fuel cell, are taken into consideration herein.

The operating costs are closely related to the operating conditions of the fuel cell. Under current experimental conditions, a mixture of 30 wt% bio-oil and 6M KOH flows through each fuel cell at a flow rate of  $4 \text{ mLmin}^{-1}$  to deliver an optimal power density of  $42.7 \text{ mWcm}^{-2}$  (Table 2). Waste bio-oil after the electrochemical reaction is not recycled for reuse in the fuel cell, and fresh bio-oil is continuously fed into the fuel cell to achieve a stable and optimal peak power density. However, a mature industrial process would recycle and reuse the spent fuel in a continuous-flow environment to improve the economic feasibility. Therefore, we first estimate the bio-oil recycling and reuse potential based on current experiments compared against the theoretical conversion.

Previous studies based on model compounds, such as glycerol and glucose, indicate that the electrocatalytic oxidation of these compounds facilitates the generation of current. The degree of oxidation determines the charge released from the reaction and the distribution of the final oxidation products. The oxidation of glycerol in an anion-exchange membrane electrocatalytic flow reactor results in a final product distribution of glycerate, tartronate, and mesoxalate,<sup>[19]</sup> with the release of 4, 8, and 10 mol electrons, respectively. In comparison to the complete oxidation of glycerol, during which all –OH and C–C bonds are cleaved and 14 mol electrons are released, the results of selective oxidation suggest a degree of oxidation ranging from 28.6 to 71.4%. The degree of oxidation is defined as the ratio of the theoretical number of electrons available for current generation to the number of electrons generated from complete oxidation. The electro-oxidation of glucose to gluconic acid exhibits a much lower degree of oxidation of 8.3%.<sup>[15,16]</sup> Although the mechanism of the electrochemical reaction is unclear for direct bio-oil fuel cells, the bio-oil sugar compounds are attributed to power generation for the base case. Levoglucosan is the primary sugar found in bio-oil employed in this study followed by cellobiosan, xylose, and galactose. The amount of levoglucosan accounts for 11.1 wt% of bio-oil, with a total sugar content of 17.6 wt%.<sup>[21]</sup> This indicates an equivalent levoglucosan concentration of 0.205 M. For the oxidation of levoglucosan in the direct bio-oil fuel cell, a 60% degree of oxidation is assumed, which is equivalent to generating 16.8 mol electrons per mol levoglucosan. With 60% levoglucosan conversion, the theoretical flow of charge (current density) is estimated to be  $137.0 \text{ Cmin}^{-1}\text{cm}^{-2}$  based on the fuel concentration, flow rate, degree of oxidation, and levoglucosan conversion. When bio-oil is recycled for multiple runs in a fixed-bed continuous-flow reactor, the current density of the fuel cell decreases as the levoglucosan conversion proceeds and its variation is considered. The results of glycerol oxidation indicate that half of the power density is delivered with a constant voltage when glycerol conversion reaches 60%.<sup>[19]</sup> The same trend is applied to the case of levoglucosan if the initial current density ( $42.7 \text{ mWcm}^{-2}$  or  $10.82 \text{ Cmin}^{-1}\text{cm}^{-2}$ ) is lowered to half with 60% conversion. Based on the average current density during the conversion process and the theoretical current density, the number of recycles of fresh bio-oil is estimated to be 17. This indicates that 4.27 g of bio-oil are re-



quired to generate electricity for 1 h using a 5 cm<sup>2</sup> laboratory-scale electrochemical reactor, and 4.79 g of KOH are dissolved for the preparation of the fuel solution. Although the KOH electrolyte is anticipated to be recovered, ideally with an efficient separation and recovery technology, a KOH consumption/make-up factor of 0.5% is still applied for the analysis.

The number of stacks required is determined by the amount of bio-oil produced annually and the bio-oil consumed by each fuel cell stack. A fuel cell lifespan of 3 years, with 7884 annual operating hours, is taken for the *n*th plant design by adapting the information for references.<sup>[23,33]</sup> Fuel cells are completely replaced with no salvage value in the end. The overall cost of biomass conversion to electricity by using fuel cells,  $C'_{TO}$ , includes the annual capital cost of bio-oil production, biomass feedstock cost, biomass delivery cost, annual capital cost of fuel cell stacks, KOH make-up cost, and biochar credit, as shown in Equation (4):

$$C'_{TO} = C'_{P0} + C_{F0} + C_{D0} + C_{E0} + C_p + C_o - Cr_{bc} \quad (4)$$

in which  $C'_{P0}$  is the annual capital cost for bio-oil production, including biomass pretreatment, pyrolysis, and bio-oil fractionation. This information is obtained by breaking down the biofuel production pathway and only taking into account the first three steps for bio-oil production.  $C_{F0}$ ,  $C_{D0}$ , and  $C_{E0}$  are the biomass feedstock cost, biomass delivery cost, and purchased electricity cost associated with bio-oil production, respectively.  $C_p$  is the annual capital cost of fuel cell stacks. A capital recovery factor of 0.386 is applied, which represents a 10% internal rate of return and 3 year lifetime for the fuel cells.  $C_o$  represents the KOH make-up cost in fuel cells.  $Cr_{bc}$  denotes the revenue credits from biochar coproduced along with bio-oil. Once each specific cost component is assessed, the MESP, also known as the cost of electricity (COE), can be calculated by dividing the total annual cost of the power generation system by the annual electricity production. When the biomass processing capacity changes, power law scaling factors of 0.7 and 1.5 are applied for the capital cost of bio-oil production and biomass delivery cost, respectively, whereas a linear scaling relationship is used for other cost components in Equation (4).

### Hybrid biomass conversion system

An overall process flow diagram of the hybrid bio-oil to biofuel and electricity system is illustrated in Figure 1. Biomass with a flow rate of 2000 MTPD is first converted into bio-oil through fast pyrolysis. By splitting a fraction of bio-oil to a biorefinery for transportation fuel production, with the remaining bio-oil flowing through fuel cell devices for electrical power generation, various scenarios of the hybrid system operations are explored. It is noted that the bio-oil/biofuel production process requires electricity input. One potential advantage of the hybrid system is to use the electricity generated onsite from electrochemical conversion for biofuel pro-

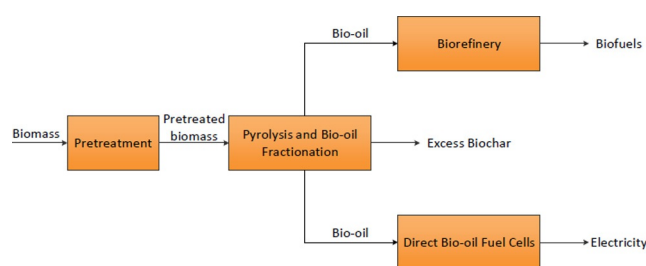


Figure 1. Process block diagram of the hybrid bio-oil to biofuel and electricity system.

duction. Due to the novelty of the direct bio-oil fuel cell technology and a wide range of energy demands under various operational conditions, the energy interaction between these two pathways is not considered, and electricity is purchased when needed for biofuel production. A general energy balance of the hybrid plant with 50% bio-oil for biofuels and 50% bio-oil for electrical power generation is chosen as an example to show its performance (Figure S1, Supporting Information).

There are different ways to evaluate the profitability of the hybrid plant with multiple products. Herein, we choose electricity as the major output product, while biofuels are considered as a coproduct sold to the market to generate excess revenue. Therefore, the MESP can be assessed based on the ratio of total annual cost of the hybrid system to the annual electricity produced. The total annual cost of the hybrid system is the summation of bio-oil production cost (with credits from biochar), biofuel production cost (bio-oil upgrading for biofuels), and electricity production cost (direct bio-oil fuel cells) minus revenue from the biofuels. This involves a cost breakdown and combination of the above-mentioned individual cost analysis method with economies-of-scale analysis because the hybrid plant includes a shared bio-oil production step and varying bio-oil upgrading capacities. The Results section compares the MESP for various fractions of bio-oil to the fuel cells.

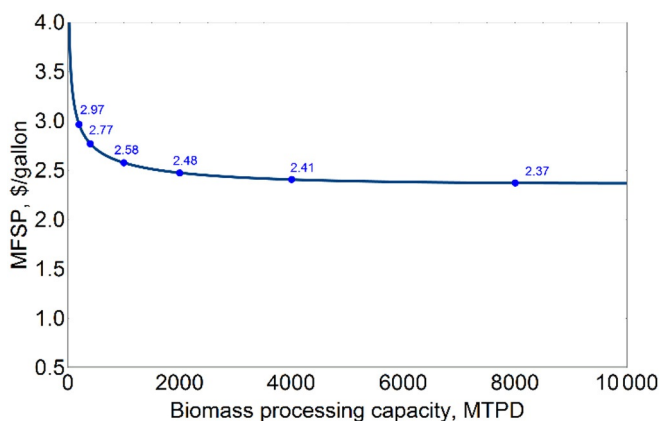
## Results

### MFSP from biofuel production

The baseline biofuel facility processes 2000 MTPD of biomass and produces 56.8 million gallons of gasoline and diesel. The costs of each component from Equation (1) and MFSP are summarized in Table 3. A MFSP of \$2.48 per gallon is calculated. The feedstock cost contributes most to the MFSP followed by other costs, which are mainly attributed to natural gas, electricity, and catalyst costs from bio-oil upgrading. Annual capital cost accounts for 22% of the total annual cost for biofuel production, whereas the feedstock delivery cost is relatively small. Upon increasing the biomass processing capacity from 200 to 10000 MTPD, a declining MFSP is observed (Figure 2). With a further increase in biomass processing capacity, a minimum value is expected, although it is not fully presented here.

**Table 3.** Breakdown of total annual cost of the biofuel production pathway.

Parameter	Value
$M_0$ [MTPD]	2000
$Q_0$ ( $\times 10^5$ gallons)	56.8
$C_{P0}$ [\$ MM]	31.35
$C_{F0}$ [\$ MM]	52.56
$C_{D0}$ [\$ MM]	4.87
$C_{E0}$ [\$ MM]	4.47
$C_{O0}$ [\$ MM]	48.19
$C_{rbc}$ [\$ MM]	0.83
MFSP [\$gallon <sup>-1</sup> ]	2.48

**Figure 2.** Biomass processing capacity versus MFSP for a fast pyrolysis biorefinery.

### MESP from direct bio-oil fuel cells

The fuel cell stack cost (without catalyst), balance of the plant, and the system assembly and testing for each stack module are \$2593.1, \$1793.0, and \$93.72, respectively, with a total value of \$4479.76. MEAs with an uncatalyzed membrane account for 79.1% of the total stack cost, followed by the stamped bipolar plates at 14.9%. The catalyst cost of a fuel cell stack is evaluated to be \$1543.5 for platinum loadings and \$7.2 for iron loadings. The results suggest that the high loading and price of platinum are responsible for the high cost. The total cost of each stack module is \$6030.46, including catalyst costs. With a net power output per stack of 2.57 kW, the system cost of each stack module on a net power output basis is estimated to be approximately \$2346kW<sup>-1</sup>, compared with \$50.41kW<sup>-1</sup> for a H<sub>2</sub> PEM fuel cell stack.

The capital costs, operating costs, and MESP are presented in Table 4 based on a 2000 MTPD biomass conversion facility for direct bio-oil fuel cell application. Each fuel cell stack takes in 586.9 tonnes of bio-oil per year and 737 stacks are required to consume the bio-oil produced annually. The cost for bio-oil production, including the capital cost, biomass cost, biomass delivery cost, and energy cost, results in a bio-oil selling price of \$176tonne<sup>-1</sup>. The substantial consumption of bio-oil for fuel cells makes bio-oil production the most significant contributor to the total annual cost. Compared with

**Table 4.** Breakdown of the total annual cost for electricity generation from the direct bio-oil fuel cell.

Parameter	Value
$M_0$ [MTPD]	2000
no. stacks (N)	737
$Q_0$ [kWh]	$1.50 \times 10^7$
$C_{P0}$ [\$ MM]	15.02
$C_{F0}$ [\$ MM]	52.56
$C_{D0}$ [\$ MM]	4.87
$C_{E0}$ [\$ MM]	4.47
$C_p$ [\$ MM]	1.72
$C_s$ [\$ MM]	2.43
$C_{rbc}$ [\$ MM]	0.83
MESP [\$kWh <sup>-1</sup> ]	5.36

bio-oil production, the cost of fuel cell stacks is very small due to the small number of fuel cell stacks needed. Operating costs of fuel cell stacks dominate the total costs, rather than the capital costs. KOH contributes significantly to the operating costs, despite a conservative make-up factor of 0.5%; this is attributed to the significant mass flow rate of KOH required to achieve the peak power density and its relatively high price. A final MESP of \$5.36kWh<sup>-1</sup> is estimated. Although the projected MESP is not yet competitive and ready for market penetration, further improvement of the performance of the fuel cell will help to drive down the cost for long-term success. A combination of factors, such as the effective reactant content in bio-oil (11.1 wt% levoglucosan), degree of oxidation of levoglucosan (0.6), and peak power density delivered (42.7 mWcm<sup>-2</sup>), are regarded to be primary drivers for the COE. Key factors and the potential for cost reduction are further explored in the following section.

### Sensitivity analysis

A number of input variables in the techno-economic model could potentially affect the COE. Key parameters, such as effective reactant content (levoglucosan), the degree of oxidation, the levoglucosan conversion factor, power density, the capital cost of the fuel cell stack, system efficiency, fuel cell lifetime, and catalyst loadings, are explored in the sensitivity analysis. Because a larger levoglucosan conversion results in a lower final power density, a specific relationship between them needs to be incorporated for the sensitivity analysis. Without updating the model with new information, the conversion factor is expected to show a similar trend to that of the degree of oxidation because they are correlated in the MESP calculation. Therefore, only the degree of oxidation is selected for analysis.

The results from Figure 3 show that the effective reactant content is the most influential factor, followed by the degree of oxidation. Levoglucosan is identified as the effective reactant for power generation. The very low concentration of levoglucosan in bio-oil (11.1 wt%) underscores the inefficiency of bio-oil utilization. Increasing the levoglucosan content in bio-oil or the amount of effective reactant content in bio-oil by 20% can result in a 16% reduction in the COE. The

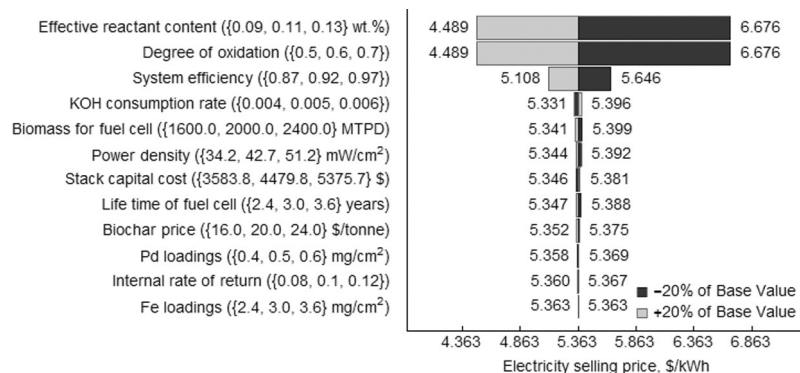


Figure 3. Sensitivity analysis of key parameters of the MESP.

degree of oxidation of levoglucosan significantly affects the electricity selling price because a higher degree of oxidation indicates larger electricity output for the same amount of bio-oil. The increase in system efficiency leads to a higher power output, and thus, a lower COE. Although a very small make-up fraction of KOH is applied, the high concentration and amount of KOH required for the electrochemical reaction make it a clear contributor to the final electricity price. The biomass conversion capacity influences the bio-oil price due to the impacts of the economies of scale, but its ultimate impact on the price of electricity is limited within the range considered. Varying the power density only changes the COE slightly, likely because the increase in power density improves both the electrical power output and bio-oil consumption, and the combination of both effects contributes to the final electricity price. The sensitivity results are consistent with the previous base-case scenario that the factors associated with the operating costs of the fuel cell system are crucial and most influential to the COE. In comparison, cost factors, such as the stack capital cost; fuel cell lifetime; and catalyst loadings contribute less.

The sensitivity results suggest that the most influential parameters can be potentially optimized to improve the economic feasibility of the direct bio-oil fuel cell technology by using future technical breakthroughs and technological advances. Figure 4 shows that the estimated MESP can be remarkably reduced to  $\$1.28\text{kWh}^{-1}$ , upon increasing the effective reactant content of levoglucosan from 11.1 to 50 wt %, as indicated in the literature.<sup>[34]</sup> With further improvements to the degree of oxidation and system efficiency, an optimal electricity selling price of  $\$0.96\text{kWh}^{-1}$  is expected. This indicates that the potential of improving the direct bio-oil fuel cell application is large and a competitive electricity selling price is achievable, in contrast to other commercial fuel cell technologies.

The impact of biomass processing capacity change on the MESP from direct bio-oil fuel cells is evaluated based on the optimal operating conditions (Figure 5). The results show that the MESP is reduced with an increase in biomass processing quantity from 200 to 4000 MTPD. A further increase in the biomass processing capacity leads to a slightly higher COE. This phenomenon is dominated by the bio-oil produc-

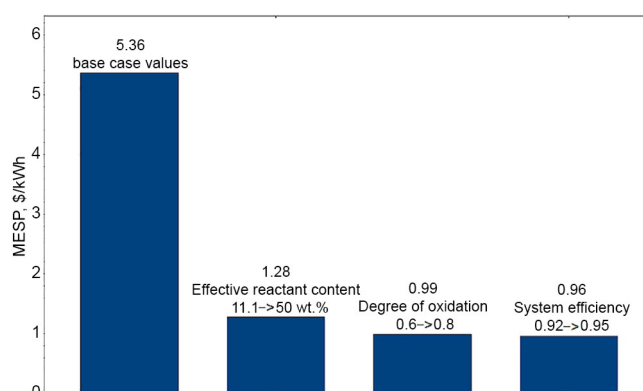


Figure 4. Potential for cost reduction of the direct bio-oil fuel cell.

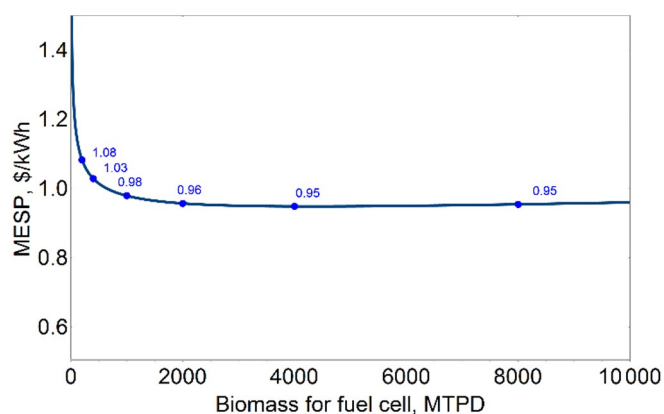


Figure 5. Effect of biomass processing capacity on the MESP of a biomass fast pyrolysis and bio-oil fuel cell power-generation system.

tion cost and combined effects of economies of scale and intrinsic characteristics of biomass delivery. Variation of the biomass processing capacity also results in a change of the total amount of bio-oil, the number of stacks, and the electrical power generated in a specific system, which thereby affects the MESP estimate.

## MESP from the hybrid system

The bio-oil stream is split into two fractions for electricity and biofuel production in the hybrid system. Various bio-oil fractions allocated for the fuel cell application are explored and compared. Based on this analysis approach for the hybrid plant, in which biofuels are considered as revenues and electricity selling prices are projected, the quantity of biofuels produced annually and the MFSP are required as input parameters. The baseline assumptions for the biofuel pathway include a bio-oil yield of 65.5 wt % on a dry biomass basis and a biofuel production rate of 86.5 gallons per tonne of biomass, as indicated in Table 1. A market biofuel MFSP of \$3 gallon<sup>-1</sup> is used for analysis.

The impact of fuel cell bio-oil fractions on the final MESP is illustrated in Figure 6, and the breakdown of cost components for different scenarios is summarized in Table 5. As the allocation of bio-oil for the fuel cell decreases from 100 to 20%, the MESP decreases from \$0.96 to  $-\$0.28\text{kWh}^{-1}$ . These results suggest that increasing revenues from biofuels outweigh decreasing sales of electricity from fuel cells. Although biofuel production costs are greater than those for electricity, the net profit for the hybrid facility increases with greater biofuel output. Furthermore, we determined that, with a bio-oil fraction of 24.2% for the fuel cell application, the electricity price approaches zero, which indicates the

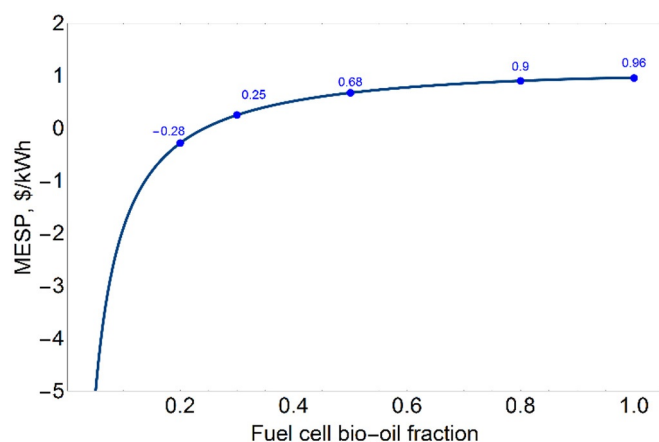


Figure 6. Impact of bio-oil fraction allocation on MESP for the hybrid bio-oil to biofuel and electricity system.

breakeven point at which the total production costs of the hybrid system, including bio-oil production cost, electricity production cost, and biofuel production cost, are equivalent to the sales revenue from biofuels. With a fuel cell bio-oil allocation fraction lower than 24.2%, the hybrid system effectively subsidizes the fuel cell power generation.

Previous discussion indicates that the variation of key parameters from the biofuel production pathway, such as the biofuel selling price and its yield, have a direct impact on the total annual cost and the MESP from the hybrid system. Because these two parameters are correlated in terms of the revenue estimate, we only take the biofuel selling price as a variable in the sensitivity analysis. Figure 7 illustrates the effect of biofuel selling prices on the MESP. A linear relationship is observed for different fuel cell bio-oil fractions. When a higher fraction of bio-oil is allocated for fuel cells, the MESP tends to be high and stable. A much higher biofuel selling price is required to achieve a target MESP. Data from the U.S. Energy Information Administration shows an industrial electricity price of 6.91 cents  $\text{kWh}^{-1}$  in 2015.<sup>[35]</sup> To make the electricity economically competitive at this price level, biofuel selling prices of \$8.58, 4.02, 3.14, and 2.87 per gallon are estimated when 80, 50, 30, and 20% of the bio-oil supply is allocated for fuel cells, respectively.

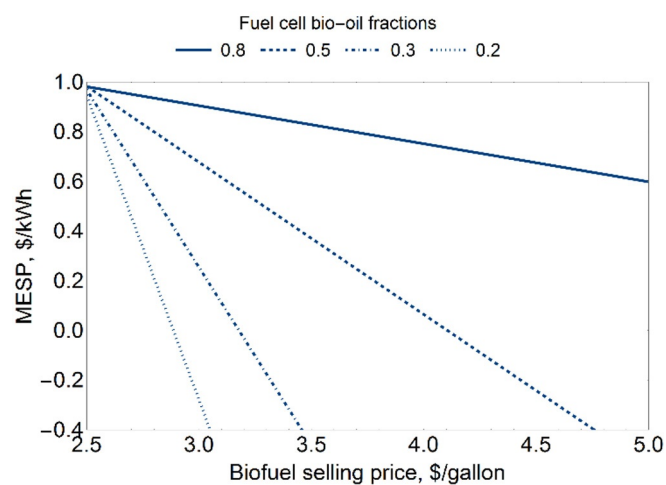


Figure 7. Impact of biofuel selling price on MESP for varying fuel cell bio-oil fractions.

Table 5. Breakdown of the cost components for specific hybrid system designs.

Fuel cell bio-oil fraction	Bio-oil production cost (with biochar credits) [\\$MM]	Electricity production cost (fuel cells) [\\$MM]	Biofuel production cost (bio-oil upgrading for biofuels) [\\$MM]	Revenue from biofuels [\\$MM]	Annual electricity production [kWh]	MESP [\$/kWh <sup>-1</sup> ]
1	76.09	12.73	0	0	$9.27 \times 10^7$	0.96
0.8	76.09	10.19	14.93	34.09	$7.42 \times 10^7$	0.90
0.5	76.09	6.37	34.15	85.21	$4.64 \times 10^7$	0.68
0.3	76.09	3.82	46.46	119.30	$2.78 \times 10^7$	0.25
0.2	76.09	2.55	52.52	136.34	$1.85 \times 10^7$	-0.28



## Conclusions

Bio-oil derived from biomass fast pyrolysis can be thermochemically upgraded to gasoline and diesel or electrochemically converted for electrical power generation. The biofuel production pathway employs typical hydrotreating and hydrocracking steps, while the electricity is generated using a direct bio-oil fuel cell technology.

This study evaluated the technoeconomics of each individual pathway with a specific focus on the direct bio-oil fuel cell application based on a 2000 tonnes per day biomass processing facility. A MFSP of \$2.48 per gallon is projected, while a MESP of \$5.36 kWh<sup>-1</sup> is estimated based on current laboratory data of the direct bio-oil fuel cell. We found that the technical performance parameters of bio-oil fuel cells, including the effective reactant content, degree of oxidation, and the system efficiency, are the most influential factors to the final electricity selling price from the sensitivity analysis. A combined improvement of these three parameters results in a lower electricity selling price of \$0.96 kWh<sup>-1</sup>. This indicates that advances in the technical performance of the novel fuel cell method could lead to commercially competitive electricity prices in the future.

The hybrid biomass conversion system allocates a portion of bio-oil for fuel cells, while the rest of the bio-oil is upgraded for drop-in biofuels production. With the assumptions that 86.5 gallons of biofuels are produced per tonne of biomass and sold at a price of \$3 per gallon, the MESP from the hybrid system decreases from \$0.96 to -\$0.28 kWh<sup>-1</sup> as the fuel cell bio-oil fraction changes from 100 to 20%. A fuel cell bio-oil fraction of less than 24.2% enables the hybrid system to be profitable, even without electricity revenue. This suggests that the current challenges associated with direct bio-oil fuel cells could be offset by revenues from the production of biofuels.

## Acknowledgements

We gratefully acknowledge financial support from the Iowa Energy Center (grant no. 4781742) and the Bioeconomy Institute at Iowa State University. We thank Neeva Benipal from the Chemical Engineering Department at Iowa State University for her detailed explanation of the experimental results.

## Conflict of interest

The authors declare no conflict of interest.

**Keywords:** biomass • electrochemistry • fuel cells • pyrolysis • technoeconomic analysis

- [1] A. A. Khan, W. de Jong, P. J. Jansens, H. Spliethoff, *Fuel Process. Technol.* **2009**, *90*, 21–50.
- [2] J. A. Ruiz, M. C. Juarez, M. P. Morales, P. Muñoz, M. A. Mendivil, *Renewable Sustainable Energy Rev.* **2013**, *18*, 174–183.
- [3] D. Chiamonti, A. Oasmaa, Y. Solantausta, *Renewable Sustainable Energy Rev.* **2007**, *11*, 1056–1086.
- [4] R. P. Anex, A. Aden, F. K. Kazi, J. Fortman, R. M. Swanson, M. M. Wright, J. A. Satrio, R. C. Brown, D. E. Dugaard, A. Platon, G. Kothandaraman, D. D. Hsu, A. Dutta, *Fuel* **2010**, *89*, S29–S35.
- [5] Q. Dang, W. Hu, M. Rover, R. C. Brown, M. M. Wright, *Biofuels Bioprod. Biorefin.* **2016**, *10*, 790–803.
- [6] H. Jhong, S. Ma, P. Kenis, *Curr. Opin. Chem. Eng.* **2013**, *2*, 191–199.
- [7] Z. Li, S. Kelkar, L. Raycraft, M. Garedew, J. E. Jackson, D. J. Miller, C. M. Saffron, *Green Chem.* **2014**, *16*, 844–852.
- [8] S. Kersten, M. Garcia-Perez, *Curr Opin Biotech* **2013**, *24*, 414–420.
- [9] D. Mohan, C. U. Pittman, P. H. Steele, *Energy Fuels* **2006**, *20*, 848–889.
- [10] Y. S. Choi, P. A. Johnston, R. C. Brown, B. H. Shanks, K. H. Lee, *J. Anal. Appl. Pyrolysis* **2014**, *110*, 147–154.
- [11] W. Hu, Q. Dang, M. Rover, R. C. Brown, M. M. Wright, *Biofuels* **2016**, *7*, 57–67.
- [12] W. Li, Q. Dang, R. Smith, R. C. Brown, M. M. Wright, *ACS Sustainable Chem. Eng.* **2017**, *5*, 1528–1537.
- [13] Q. Dang, M. Wright, R. C. Brown, *Environ. Sci. Technol.* **2015**, *49*, 14688–14695.
- [14] C. H. Lam, S. Das, N. C. Erickson, C. D. Hyzer, M. Garedew, J. E. Anderson, T. J. Wallington, M. A. Tamor, J. E. Jacksonae, C. M. Saffron, *Sustainable Energy Fuels* **2017**, *1*, 258–266.
- [15] N. Fujiwara, S. Yamazaki, Z. Siroma, T. Ioroi, H. Senoh, K. Yasuda, *Electrochem. Commun.* **2009**, *11*, 390–392.
- [16] D. Basu, S. Basu, *Electrochim. Acta* **2010**, *55*, 5775–5779.
- [17] Z. Zhang, L. Xin, J. Qi, D. J. Chadderdon, W. Li, *Appl. Catal. B* **2013**, *136*, 29–39.
- [18] L. An, T. Zhao, S. Shen, Q. Wu, R. Chen, *J. Power Sources* **2011**, *196*, 186–190.
- [19] J. Qi, L. Xin, D. J. Chadderdon, Y. Qiu, Y. Jiang, N. Benipal, C. Liang, W. Li, *Appl. Catal. B* **2014**, *154*, 360–368.
- [20] Z. Zhang, L. Xin, J. Qi, D. J. Chadderdon, K. Sun, K. M. Warsko, W. Li, *Appl. Catal. B* **2014**, *147*, 871–878.
- [21] N. Benipal, J. Qi, P. A. Johnston, J. C. Gentile, R. C. Brown, W. Li, *Fuel* **2016**, *185*, 85–93.
- [22] H. Tsuchiya, O. Kobayashi, *Int. J. Hydrogen Energy* **2004**, *29*, 985–990.
- [23] D. B. Nelson, M. H. Nehrir, C. Wang, *Renewable Energy* **2006**, *31*, 1641–1656.
- [24] M. F. Sgroi, F. Zedde, O. Barbera, A. Stassi, D. Sebastián, F. Lufrano, V. Baglio, A. S. Aricò, J. L. Bonde, M. Schuster, *Energies* **2016**, *9*, 1008.
- [25] S. Jones, P. Meyer, L. Snowden-Swan, A. Padmaperuma, E. Tan, A. Dutta, J. Jacobson, K. Cafferty, *Technical Report: PNNL-23053; NREL/TP-5100-61178*, US Department of Energy, Oak Ridge, TN, **2013**.
- [26] A. Dutta, A. Sahir, E. Tan, D. Humbird, L. J. Snowden-Swan, P. Meyer, J. Ross, D. Sexton, R. Yap, J. Lukas, *Technical Report: NREL/TP-5100-62455, PNNL-23823*, US Department of Energy, Oak Ridge, TN, **2015**.
- [27] M. Wright, R. C. Brown, *Biofuels Bioprod. Biorefin.* **2007**, *1*, 191–200.
- [28] R. M. Darling, K. G. Gallagher, J. A. Kowalski, S. Ha, F. R. Brushett, *Energy Environ. Sci.* **2014**, *7*, 3459–3477.
- [29] B. M. Jenkins, *Biomass Bioenergy* **1997**, *13*, 1–9.
- [30] B. D. James, J. A. Kalinoski, K. N. Baum, *Manufacturing Cost Analysis of Fuel Cell Systems*, Directed Technologies Inc., **2010**.
- [31] Alibaba, Price for potassium hydroxide, [https://www.alibaba.com/trade/search?fsb=y&IndexArea=product\\_en&CategoryId=&Search-Text=potassium+hydroxide+price&isGalleryList=G&viewtype=G](https://www.alibaba.com/trade/search?fsb=y&IndexArea=product_en&CategoryId=&Search-Text=potassium+hydroxide+price&isGalleryList=G&viewtype=G), accessed 10 January 2017.
- [32] Carolina Company, Price for Iron, [http://www.carolina.com/catalog/detail.jsp?prodId=869240&s\\_cid=ppc\\_products&utm\\_source=google&utm\\_medium=cpc&s\\_cid=ppc\\_gl\\_products&scid=scplp869240&sc\\_intid=869240&clid=Cj0KEQIA5IHEBRCL\\_](http://www.carolina.com/catalog/detail.jsp?prodId=869240&s_cid=ppc_products&utm_source=google&utm_medium=cpc&s_cid=ppc_gl_products&scid=scplp869240&sc_intid=869240&clid=Cj0KEQIA5IHEBRCL_)

- PZvq2\_6qcBEiQAL4cQ09onycWkYKalyW4uPkf9wPSOdi0aE-ja7UmxC4plegUkaArOr8P8HAQ, accessed 10 January 2017.
- [33] DOE, *Fuel Cells*, <https://energy.gov/eere/fuelcells/fuel-cells>, accessed 10 January 2017.
- [34] M. B. Shemfe, S. Gu, P. Ranganathan, *Fuel* **2015**, *143*, 361–372.
- [35] EIA, *Average Price of Electricity to Ultimate Customers*, [https://www.eia.gov/electricity/monthly/epm\\_table\\_grapher.cfm?t=epmt\\_5\\_3](https://www.eia.gov/electricity/monthly/epm_table_grapher.cfm?t=epmt_5_3), accessed 10 January 2017.

---

Manuscript received: June 18, 2017

Revised manuscript received: September 5, 2017

Accepted manuscript online: September 7, 2017

Version of record online: November 16, 2017